

3. Dybkowski M. Industrial Drive Systems. Current State and Development Trends // Ind. Drive Syst. Curr. State Dev. Trends. – 2016. – Vol. 1, No. 1. – P. 5–25. – DOI: 10.5277/ped160101.

4. Parmar C.A., Ami P. Speed Control Technique for Induction Motor // A Review. – 2014. – Vol. 2, No. 08. – P. 236–238.

5. Akhila V.T., Arun S. Review of Solar PV Powered Water Pumping System Using Induction Motor Drive // IOP Conf. Ser. Mater. Sci. Eng. – 2018. – Vol. 396, No. 1. – DOI: 10.1088/1757-899X/396/1/012047.

6. Amézquita-Brooks L.A., Licéaga-Castro J., Licéaga-Castro E., Ugalde-Loo C.E. Induction Motor Control: Multivariable Analysis and Effective Decentralized Control of Stator Currents for High-Performance Applications // IEEE Trans. Ind. Electron. – 2015. – Vol. 62, No. 11. – P. 6818–6832. – DOI: 10.1109/TIE.2015.2436360.

UDC 621.391.825

## QUASISTATIC SIMULATION OF REFLECTION SYMMETRIC MEANDER LINE WITH THREE CONDUCTORS CONNECTED AT ONE END

*E.B. Chernikova, postgraduate student,*

*Department of Television and Control*

*Scientific adviser A.M. Zabolotsky, DScTech, professor*

*Tomsk, Tomsk State University of Control Systems and Radioelectronics,*

*chernikova96@mail.ru*

The article considers two connection diagrams for a reflection symmetric meander line with the length  $l=1$  m, in which three conductors are connected at one end. Quasi-static simulation of the diagrams under consideration with optimal parameter values was performed. The results of the work could be used to improve the devices protecting against ultra-short pulses.

**Keywords:** electromagnetic compatibility, protection device, ultrashort pulse, modal filtration, reflection symmetric meander line.

In the modern world there is a tendency to tighten the requirements for ensuring electromagnetic compatibility (EMC) of radio-electronic equipment (REE). A separate task of EMC is the protection of REE from electromagnetic interference [1]. Ultrashort pulses (USP) [2] that have short duration and wide spectrum and penetrate into REE through signal conductors or through power circuits represent a particular danger. A modal filtration technique has been proposed [3], which consists in the decomposition of a USP into a sequence of lower amplitude pulses in structures with inhomogeneous dielectric filling caused by the difference in mode delays.

Various configurations of such structures have been investigated, including structures with reflection symmetry [4]. Meanwhile, the possibility

of decomposing a USP in a reflection symmetric meander line (ML) (Fig. 1) with three conductors connected at one end has not been previously considered, although this is relevant. The purpose of this work is to carry out such research.

The simulation of the studied ML with a length ( $l$ ) of 1 m was performed using the quasi-static approach in the TALGAT software [5]. To simulate the time response, we used a source of pulsed signals represented by an ideal source of EMF with an amplitude of 5 V with rise time, fall and flat top durations of 50 ps each, so  $t_{\Sigma}$  is 150 ps. The half-turn connection diagrams are shown in Fig. 2. The simulation of the ML was carried out with the optimized parameters of the cross-section from [6], which ensure the equality of the time intervals between the per-unit-length delays of the modes and the pairwise equalized amplitudes of the output signal voltages.

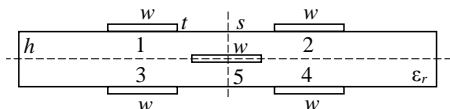


Fig. 1. Cross-section of the reflection symmetric structure

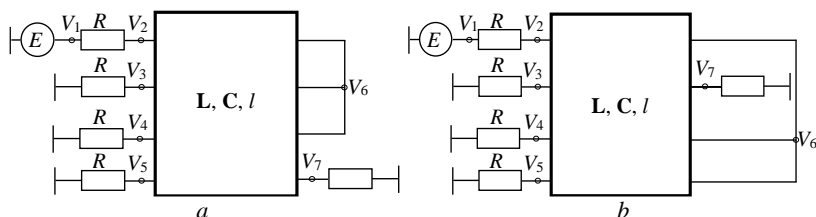


Fig. 2. Connection diagrams of the MLs under study: 1 (a) and 2 (b)

The voltage waveforms at the ML outputs (nodes  $V_3$ ,  $V_4$  in Fig. 2, a and nodes  $V_4$ ,  $V_5$  in Fig. 2, b) are shown in Fig. 3 and 4, respectively. The table below summarizes the values of the modes 1–4 per-unit-length delays multiplied by 1 and 2.

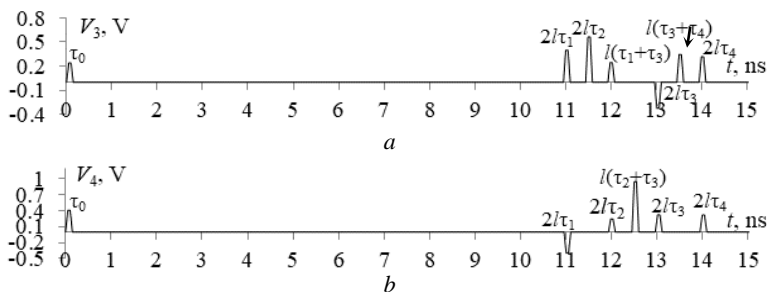


Fig. 3. Voltage waveforms at the diagram 1 output: node  $V_3$  (a) and node  $V_4$  (b)

In Figs. 3 and 4 we can see the appearance of additional pulses, whose delays are equal to a mode delay multiplied by 1, among the main pulses, whose delays are different. This can be seen explicitly only for diagram 1 at node  $V_3$ . To detect additional pulses for diagram 2 at node  $V_5$ , as well as for diagram 1 (node  $V_4$ ) and 2 (node  $V_4$ ), we calculated the time response with increasing  $h$  to  $1000 \mu\text{m}$  (Fig. 5).

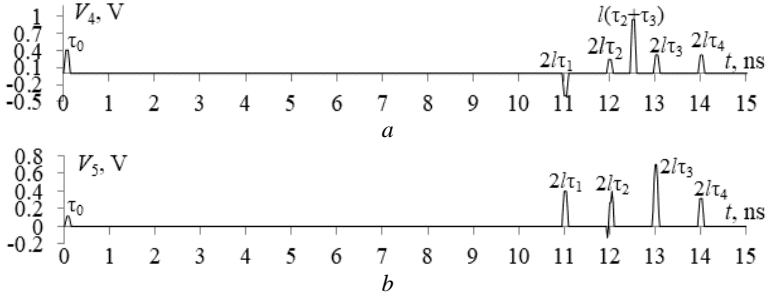


Fig. 4. Voltage waveforms at the diagram 2 output: node  $V_4$  (a) and node  $V_5$  (b)

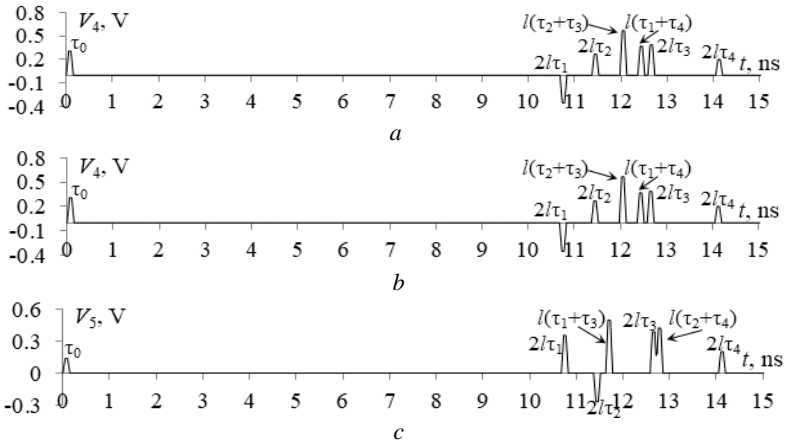


Fig. 5. Voltage waveforms at the output of the diagrams: 1, node  $V_4$  (a) and 2, nodes  $V_4$  (b) and  $V_5$  (c) at  $h=1000 \mu\text{m}$

**Values of per-unit-length pulse delays (ns/m) for modes 1–4 multiplied by 1 and 2**

Multiplier	1	2	3	4
1 ( $h = 500 \mu\text{m}$ )	5.47587	5.96472	6.47973	6.97027
2 ( $h = 500 \mu\text{m}$ )	10.9517	11.9294	12.9595	13.9405
1 ( $h = 1000 \mu\text{m}$ )	5.33958	5.68527	6.29027	7.02351
2 ( $h = 1000 \mu\text{m}$ )	10.6792	11.3705	12.5805	14.047

Thus, from the analysis of the table and Figs. 3–5 it follows that the delays of additional pulses are equal to the arithmetic mean value of doubled per-unit-length delays of the two modes (or simply the sum of per-unit-length delays) in different versions, multiplied by 1. For diagram 1 (nodes  $V_3$  and  $V_4$ ), these delays are equal to  $l(\tau_1 + \tau_3) = 11.955$  ns/m;  $l(\tau_3 + \tau_4) = 13.45$  ns/m and  $l(\tau_2 + \tau_3) = 11.975$  ns/m;  $l(\tau_1 + \tau_4) = 12.363$  ns/m, respectively. For diagram 2 (nodes  $V_4$  and  $V_5$ )  $l(\tau_2 + \tau_3) = 11.975$  ns/m;  $l(\tau_1 + \tau_4) = 12.36$  ns/m and  $l(\tau_1 + \tau_3) = 11.625$  ns/m;  $l(\tau_2 + \tau_4) = 12.708$  ns/m, respectively. But due to the symmetry, the delays of additional pulses can coincide with each other (as in diagrams 1 and 2, nodes  $V_4$ ) or with the main ones (as in diagram 2, node  $V_5$ ).

The reported study was funded by Russian Science Foundation (project №20-19-00446) in TUSUR.

### REFERENCES

1. Radasky W.A., Baum C.E., Wik M.W. Introduction to the special issue on High-Power Electromagnetics (HPEM) and Intentional Electromagnetic Interference (IEMI) // Special issue of IEEE Transactions on Electromagnetic Compatibility. – 2004. – Vol. 46, No. 3. – P. 314–321.
2. Mora N., Vega F., Lugrin G., Rachidi F., Rubinstein M. Study and classification of potential IEMI sources // System and assessment notes. – Note 41. – 8 July 2014.
3. Gazizov A.T., Zabolotsky A.M., Gazizov T.R. UWB pulse decomposition in simple printed structures // IEEE Transactions on Electromagnetic Compatibility. – 2016. – Vol. 58, No. 4. – P. 1136–1142.
4. Belousov A.O., Chernikova E.B., Samoylichenko M.A., Medvedev A.V., Nosov A.V., Gazizov T.R. and Zabolotsky A.M. From symmetry to asymmetry: the use of additional pulses to improve protection against ultrashort pulses based on modal filtration // Symmetry. – 2020. – Vol. 12 (7), No. 1117. – P. 1–38.
5. Kuksenko S.P. Preliminary results of TUSUR University project for design of spacecraft power distribution network: EMC simulation // IOP Conf. Series: Materials Science and Engineering. – 2019. – Vol. 560, No. 012110. – P. 1–7.
6. Chernikova E.B., Belousov A.O., Gazizov T.R., Zabolotsky A.M. Using reflection symmetry to improve the protection of radio-electronic equipment from ultrashort pulses // Symmetry. – 2019. – Vol. 11(7), No. 883. – P. 1–25.